

# The Secreted Ly6/uPAR-Related Protein-1 (SLURP1) Protects the Cornea From Oxidative Stress

Satinder Kaur,\* Peri Sohnen, Simran Kumar, Mehak Vohra,\*\* Sudha Swamynathan, and Shivalingappa Swamynathan

Department of Ophthalmology, Morsani College of Medicine, University of South Florida, United States

Correspondence: Shivalingappa Swamynathan, Department of Ophthalmology, Morsani College of Medicine, University of South Florida, 12901 Bruce B. Downs Blvd., Room 2114, Tampa, FL 33612, USA; [SS65@USF.edu](mailto:SS65@USF.edu).

SK and PS contributed equally to this work.

Current affiliation: \*Department of Ophthalmology, Stanford University, CA, USA.

Current affiliation: \*\*Dr. Shroff's Charity Eye Hospital, New Delhi, India.

**Received:** October 1, 2024

**Accepted:** February 20, 2025

**Published:** March 17, 2025

Citation: Kaur S, Sohnen P, Kumar S, Vohra M, Swamynathan Sudha, Swamynathan Shivalingappa. The secreted Ly6/uPAR-related protein-1 (SLURP1) protects the cornea from oxidative stress. *Invest Ophthalmol Vis Sci.* 2025;66(3):30. <https://doi.org/10.1167/iovs.66.3.30>

**PURPOSE.** Previously, we reported that the secreted Ly6/uPAR-related protein-1 (SLURP1), abundantly expressed by the corneal epithelium (CE) and secreted into the tear fluid, suppresses NF- $\kappa$ B signaling in healthy corneas and is downregulated in response to a variety of stressors, allowing helpful inflammation to progress. Here we investigate whether SLURP1 manifests its broad protective effects by promoting corneal redox homeostasis.

**METHODS.** Oxidative stress was induced in the wild-type (WT) and *Slurp1*-null (*Slurp1X*<sup>-/-</sup>) mouse corneas using 1350 J/m<sup>2</sup> UV-B, and in human corneal limbal epithelial (HCLE) and SLURP1-overexpressing HCLE-SLURP1 cells with 100 J/m<sup>2</sup> UV-B, 0.4  $\mu$ g/mL mitomycin-C, or 0–100  $\mu$ M H<sub>2</sub>O<sub>2</sub>. We evaluated their (i) redox status (GSH:GSSG ratio) using O-phthalaldehyde; (ii) reactive oxygen species (ROS) accumulation using 2',7'-dichlorodihydrofluorescein diacetate; (iii) antioxidants *GPX4*, *CAT*, and *SOD2* expression by qRT-PCR; (iv) lipid peroxidation by staining for 4-hydroxynonenol, malondialdehyde, and BODIPY-C11; and (v) DNA damage and NF- $\kappa$ B activation by immunostaining for  $\gamma$ H2AX, 8-OHdG, NF- $\kappa$ B, and I $\kappa$ B.

**RESULTS.** *Slurp1* was significantly downregulated in the UV-B-irradiated WT corneas. Oxidatively stressed HCLE-SLURP1 cells displayed relatively less ROS accumulation, lipid peroxidation, DNA damage and NF- $\kappa$ B activation, and a higher GSH/GSSG ratio and antioxidant gene expression than the similarly treated control HCLE cells. UV-B-irradiated *Slurp1X*<sup>-/-</sup> corneas displayed relatively more ROS accumulation, DNA damage and less *GPX4* expression than the similarly treated WT corneas.

**CONCLUSIONS.** Collectively, these results elucidate that SLURP1 serves as an insult-agnostic immunomodulator that upregulates antioxidants and suppresses ROS accumulation to promote redox homeostasis in corneal epithelial cells and protect them from diverse genotoxic stressors.

**Keywords:** SLURP1, ocular surface, cornea, UV-B, oxidative stress, reactive oxygen species, redox homeostasis, lipid peroxidation, DNA damage

The cornea, the anterior-most cellular layer of the eye, is a transparent, refractive tissue that acts as a barrier that protects the rest of the eye from environmental insults.<sup>1</sup> Because of its position, the cornea is exposed to high levels of solar ultraviolet (UV) radiation, microbial pathogens, and accidental chemical burns that generate high levels of reactive oxygen species (ROS) and oxidative stress.<sup>2</sup> Chronic oxidative stress causes severe injury to cornea such as photokeratitis, corneal epithelial injury, corneal edema, and opacification.<sup>3</sup> At the cellular level, oxidative stress damages mitochondrial DNA (mtDNA), nuclear DNA, cellular lipids, and proteins, culminating in cell death.<sup>4,5</sup> Excess free radicals can also trigger inflammation through activation of the nuclear factor kappa B (NF- $\kappa$ B) pathway.<sup>6,7</sup> The cornea counteracts this damage with an antioxidant defense system comprised of nonenzymatic compounds glutathione (GSH), ascorbic acid, uric acid,  $\alpha$ -tocopherol, nicotinamide-adenine dinucleotide phosphate, ferritin and coenzyme-Q10, and

enzymatic antioxidants such as catalase (CAT), superoxide dismutase (SOD), and glutathione peroxidase (GPX).<sup>7</sup> Additionally, corneal crystallins ALDH3A1 and ALDH1A1 protect ocular tissues from UV- and ROS-induced damage by virtue of their catalytic and non-catalytic functions.<sup>7,8</sup> Oxidative stress occurs when ROS accumulation surpasses the antioxidant defense capacity, contributing to inflammation and cellular damage associated with various ocular surface disorders including dry eye disease.<sup>9</sup>

The secreted Ly6/uPAR-related protein 1 (SLURP1) is a member of the Ly6/urokinase-type plasminogen activator receptor (uPAR) protein family.<sup>10,11</sup> It plays key roles in intracellular signal transduction, cell adhesion, immune activation, and serves as a tumor suppressor.<sup>12,13</sup> SLURP1 is found in various bodily fluids, including saliva, sweat, plasma, tears, and urine.<sup>14</sup> SLURP1 is highly expressed in the corneal epithelium (CE) and is secreted into tear fluid, where it acts as an immunomodulatory peptide.<sup>10</sup> Slurp1 activates

mast cells and alters cytokine production in the mouse skin.<sup>15</sup> It is a pro-differentiation factor that stalls G1-S transition during corneal epithelial cell proliferation,<sup>16</sup> modulates corneal homeostasis by scavenging urokinase-type plasminogen activator (uPA),<sup>17</sup> inhibits leukocyte infiltration in healthy corneas, prevents human umbilical vein endothelial cells tube formation,<sup>18</sup> and suppresses neutrophil chemotaxis and transmigration through endothelial cell monolayers.<sup>19</sup>

Slurp1 serves as an agonist for  $\alpha 7$  nicotinic acetylcholine receptor facilitating immune homeostasis.<sup>20–22</sup> Slurp1 expression is downregulated during alkali burn- or suture-induced corneal neovascularization, both of which induce oxidative stress,<sup>23</sup> which upregulates the expression of fibrinolytic system components PAI-1, u-PAR, t-PA and u-PA.<sup>24</sup> Previously, we reported that Slurp1 (i) serves as an immunomodulatory molecule in the mouse cornea<sup>10</sup>; (ii) expression is downregulated in cells exposed to a wide range of oxidative stressors including bacterial lipopolysaccharides, fungal zymosan-A, Pam3CSK4, pathologic conditions such as dry eye disease, microbial infections, and alkali burn<sup>10,11,25</sup>; (iii) decreases TNF- $\alpha$ -induced cytokine production and stabilizes epithelial cell junctions<sup>10,26,27</sup>; and (iv) -null (*Slurp1X*<sup>-/-</sup>) corneas display constitutively hyperactive NF- $\kappa$ B signaling and elevated angiogenic inflammation on silver nitrate cautery.<sup>26</sup> These findings and the fact that ROS accumulation is elevated in response to the proinflammatory oxidative stressors that downregulate Slurp1 expression<sup>2,7,11,23</sup> together support the hypothesis that “SLURP1 serves as an insult-agnostic immunomodulator by regulating redox homeostasis in corneal epithelial cells, thereby protecting the cornea from diverse genotoxic stressors.” In this study, we used in vitro and in vivo approaches to test this hypothesis and elucidate that SLURP1 protects the cornea from genotoxic oxidative damage by elevating the production of antioxidants and suppressing ROS accumulation.

## MATERIAL AND METHODS

### Cell Culture

Human corneal limbal epithelial (HCLE) cells and HCLE-SLURP1 cells<sup>17</sup> were cultured in keratinocyte-serum free medium (Gibco, Waltham, MA, USA) supplemented with 0.3 M CaCl<sub>2</sub>, 0.2 ng/ml epidermal growth factor and brain pituitary extract. These cells in mid-log phase of growth were treated with 100 J/m<sup>2</sup> 310 nm UV-B radiation using the UV-2 ultraviolet irradiation system (Tyler Research Corporation, Edmonton, Canada), mitomycin-C (MM-C; 0.4  $\mu$ g/ml) or increasing concentration of hydrogen peroxide (H<sub>2</sub>O<sub>2</sub>; 0–100  $\mu$ M).

### Animals

The *Slurp1X*<sup>-/-</sup> mice with a point mutation in exon 2 of the *Slurp1* gene were generously provided by Dr. Stephen Young at UCLA.<sup>28</sup> All animal studies were conducted in accordance with the ARVO statement for the use of animals in ophthalmic and vision research and adhered to the guidelines established by the University of South Florida Institutional Animal Care and Use Committee (IACUC Protocol no.: IS00011452). For all the experiments, eight-week-old C57Bl/6J wild-type and *Slurp1X*<sup>-/-</sup> mice were anesthetized with a mixture of 2% isoflurane and 1% oxygen and exposed to a single dose of 1350 J/m<sup>2</sup> UV-B radiation.

## Measurement of Reduced (GSH) to Oxidized (GSSG) Glutathione Ratio

We used GSH/GSSG ratio as a measure of oxidative stress, wherein a higher ratio indicates better redox homeostasis.<sup>29</sup> GSH and GSSG levels were determined by the O-phthalaldehyde (OPT) fluorometric method, with standard curves generated from known concentrations of GSH and GSSG.<sup>30</sup> HCLE and HCLE-SLURP1 cells at 70% confluence in six-well plates were exposed to UV-B and allowed to recover for 24 hours before measuring the GSH/GSSG ratio. Untreated cells were used as controls. The cells were harvested and homogenized in 0.1M phosphate buffer (pH 8.0) containing 5 mM EDTA and 25% metaphosphoric acid, and spun in a centrifuge at 10,000g for 1 minutes. GSH was quantified by mixing 10  $\mu$ L of the supernatant with 180  $\mu$ L phosphate buffer and 10  $\mu$ L of OPT, incubating at room temperature (RT) for 15 minutes, and measuring fluorescence with excitation and emission at 350 and 420 nm, respectively. To measure GSSG in the cell lysate, GSH was quenched by mixing 20  $\mu$ L of the supernatant with 5  $\mu$ L 0.04 M N-ethylmaleimide and incubating at RT for 30 minutes. Then, 25  $\mu$ L of the GSH-quenched cell lysate was mixed with 175  $\mu$ L of 0.1 M NaOH and 10  $\mu$ L of OPT, incubated for 15 minutes at RT, and fluorescence was measured with excitation and emission at 350 nm and 420 nm, respectively, using a Biotek H1 microplate reader and Gen5 software version 3.14 (Biotek, Winooski, VT, USA). To evaluate the GSH/GSSG ratio in mouse corneas, the eyeballs of untreated and UV-B-treated WT and *Slurp1X*<sup>-/-</sup> mice were enucleated after one hour of UV-B treatment, cornea was dissected, homogenized for two minutes in 0.1M phosphate buffer (pH 8.0) containing 5 mM EDTA and 25% metaphosphoric acid. The corneal lysate was then processed in the same manner as the cell culture lysate described above.

## RNA Extraction, Reverse Transcription, and Quantitative Real-Time PCR (qRT-PCR)

Total RNA was extracted using Bio Basic RNA isolation kit (for cells) or Qiagen RNA purification kit (for mouse corneas), following the manufacturer's instructions and quantified using a NanoDrop ND-1000 spectrophotometer. The cDNA synthesis was carried out using Moloney Murine Leukemia Virus reverse transcriptase (Promega, Madison, WI, USA). The qRT-PCR was conducted using TATA-box binding protein as endogenous control (QuantStudio 3, Applied Biosystems, Waltham, MA, USA). Expression levels of human *GPX4*, *CAT* and *SOD2*, and mouse *Gpx4*, *Cat*, and *Sod2* were quantified in UV-B exposed HCLE, HCLE-SLURP1-7, and HCLE-SLURP1-14 cells, and WT and *Slurp1X*<sup>-/-</sup> mouse corneas, respectively. The results were analyzed by the comparative threshold cycle (Ct) method and normalized by TATA-box binding protein expression. Oligonucleotide sequences of the primers used are given in Supplementary Table S1.

## Measurement of Intracellular ROS Accumulation

Intracellular ROS accumulation was measured using H<sub>2</sub>DCFDA (2',7'-dichlorodihydrofluorescein diacetate) assay kit (cat no. 10058; Biotium, Fremont, CA, USA) according to manufacturer's protocol. H<sub>2</sub>DCFDA, a cell-permeable fluorogenic dye, is deacetylated by cellular esterases to a nonfluorescent compound and later oxidized by ROS into highly

fluorescent 2',7'-dichlorofluorescein (DCF). HCLE, HCLE-SLURP1-7, and HCLE-SLURP1-14 cells were seeded in 96-well black polystyrene plates with clear bottom (Corning Inc., Corning, NY, USA) at 10,000 cells/well and incubated for 18 hours. Cells were washed with 1× PBS, stained with 10 μM H<sub>2</sub>DCFDA for 30 minutes at 37°C, washed with 1X PBS, exposed to UV-B or 0–100 μM H<sub>2</sub>O<sub>2</sub> or 0.4 μg/ml MM-C, and fluorescence was measured with excitation and emission set at 485 nm and 535 nm, respectively. DCF fluorescence was normalized to crystal violet stain absorbance to account for differences in cell numbers and expressed as fold change relative to untreated HCLE controls.

For evaluating the effect of exogenous SLURP1 on ROS production, HCLE cells were grown in conditioned medium (CM) from HCLE, HCLE-SLURP1-7 and HCLE-SLURP1-14 cells. Alternatively, HCLE cells were grown in culture medium containing increasing amounts of recombinant 6XHis-SLURP1 expressed in *Pichia pastoris* and partially purified in house using Ni-ion affinity column chromatography.<sup>19</sup> The control protein used in these assays was mock purified in a similar manner from the parental strain of *Pichia* lacking SLURP1-expressing vector. This was followed by UV-B treatment and H<sub>2</sub>DCFDA assay as above. To assess ROS levels in mouse corneas, WT and *Slurp1X*<sup>-/-</sup> mice were exposed to UV-B radiation (1350 J/m<sup>2</sup>), and after one hour, their eyeballs were enucleated and collected in PBS. The corneas were dissected, homogenized in 100 μL PBS, spun in a centrifuge at 10,000g for five minutes, and 50 μL of the supernatant was analyzed for H<sub>2</sub>DCFDA assay.<sup>31</sup>

### Immunofluorescent Staining

HCLE and HCLE-SLURP1 cells were seeded on glass coverslips coated with collagen. At 70% confluence, the cells were exposed to UV-B radiation (100 J/m<sup>2</sup>) and allowed to recover for 24 hours. The cells on coverslips were fixed in 4% paraformaldehyde (PFA) in PBS for 20 minutes, washed thrice with PBS for five minutes each, permeabilized with 0.1% Triton X-100 in PBS for two minutes, washed thrice in PBS for two minutes each, blocked in 10% donkey serum in PBS for 1.5 hours at RT, incubated with appropriate primary antibody against NFκB, IκB, 4-hydroxynonenal (4-HNE), malondialdehyde (MDA), 8-hydroxy-2'-deoxyguanosine (8-OHdG) or γ-H2AX in a humidified chamber at 4°C, washed thrice with PBS, incubated with secondary antibody and 4',6-diamidino-2-phenylindole (DAPI) for one hour at RT, and washed thrice with PBS+ 0.1% Tween-20 (PBST) for five minutes each. The coverslips were mounted using Aqua Mount (Polysciences, Warrington, PA, USA), allowed to dry overnight in the dark, sealed using clear nail polish and imaged using Keyence BZ-X800 microscope (Keyence, Itasca, IL, USA).

For mouse corneas, 8-μm-thick cryosections from freshly enucleated eyeballs embedded in optimal cutting temperature compound were fixed in 4% PFA for 10 minutes, permeabilized in PBS with 0.1% Triton for five minutes, quenched in 1% glycine for 30 minutes, blocked in 10% donkey serum for one hour at RT, incubated overnight with anti-γ-H2AX at 4°C, stained with secondary antibody and DAPI for one hour, washed three times with PBST for 10 minutes each, coverslips were mounted using Aqua Mount and allowed to dry overnight in the dark at RT. The coverslips were sealed using clear nail polish and imaged using Keyence BZ-X800

fluorescence microscope. Antibody details are provided in Supplementary Table S2.

### Measurement of Lipid Peroxidation

Untreated and UV-B treated HCLE and HCLE-SLURP1 cells were incubated with 2 μM BODIPY 581/591 C11 dye for 20 minutes. The cells were then rinsed three times with 1× PBS, fixed in 4% PFA for 20 minutes, and washed three additional times with 1× PBS for 10 minutes each. Coverslips were mounted using Aqua Mount, sealed with nail polish the next day, and imaged under red and green channels to detect the fluorescence emission shift from red (~590 nm) to green (~510 nm). Mean fluorescence intensity was analyzed using ImageJ for a ratiometric comparison of oxidized to non-oxidized states.

### Quantification of SLURP1 by Enzyme-Linked Immunosorbent Assay (ELISA)

ELISA was performed by coating high-binding 96 well plates with conditioned medium from HCLE, HCLE-SLURP1-7 or HCLE-SLURP1-14 cells, blocking for 1 hour with 4% milk in PBST at 37°C, and incubating with anti-human SLURP1 antibody (2 μg/mL; Abnova, Taipei, Taiwan) at 37°C for two hours. After washing four times each for one minute with PBST, horseradish peroxidase-conjugated anti-rabbit IgG (1:500 dilution) was added and incubated at 37°C for one hour, washed five times with PBST, and the bound antibody quantified using peroxidase substrate tetramethylbenzidine by measuring absorbance at 450 nm using a plate reader (Biotek). SLURP1 concentration was then estimated using a standard curve generated by coating increasing amounts of recombinant SLURP1 (Abnova) in duplicate in the same plate and processing as above.

### Statistical Analysis

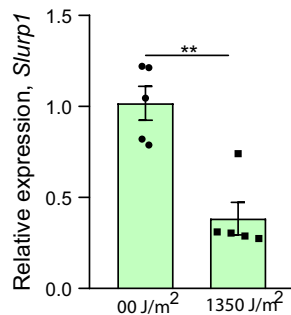
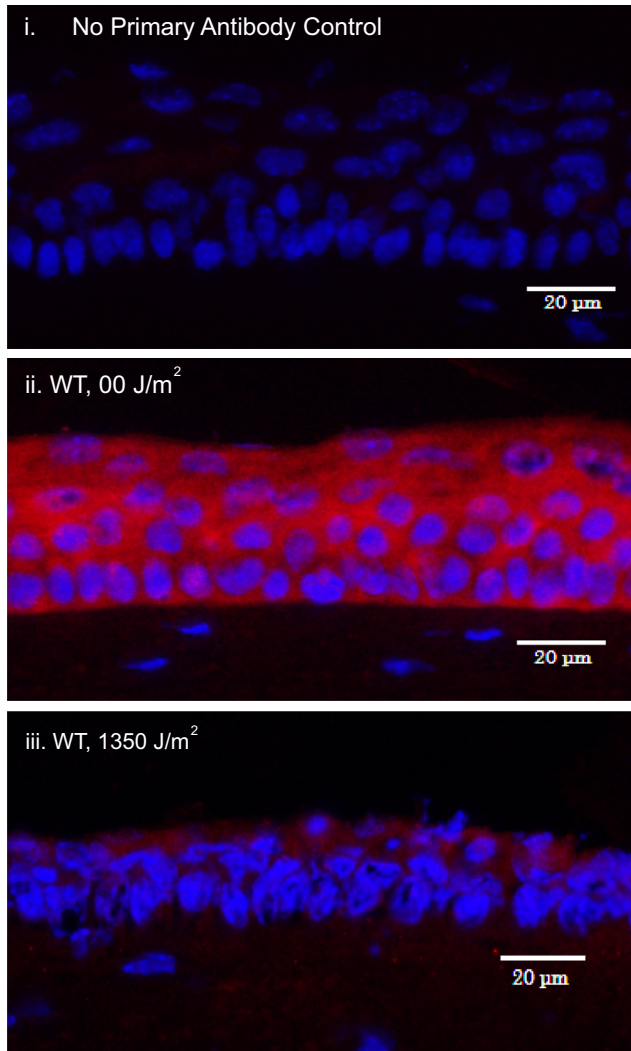
All experiments were conducted three times and representative data or mean values from all three experiments are presented along with error bars representing the standard error of the mean (SEM). For animal studies, each group consisted of five mice, and unpaired *t*-testing was used to compare *Slurp1* gene expression levels between untreated and UV-B treated WT mouse corneas. Differences between various cell lines and treatment groups were analyzed using two-way ANOVA, followed by Tukey's multiple comparisons test. A *P* value <0.05 was considered statistically significant.

## RESULTS

### *Slurp1* Is Downregulated in UV-B Irradiated WT Corneas

Previously, we demonstrated that *Slurp1* expression is downregulated in response to herpes simplex virus infection, bacterial lipopolysaccharides injection,<sup>10</sup> silver nitrate cautery burn,<sup>26</sup> exposure to Pam3CSK4, Poly(I:C), and Zymosan-A.<sup>11</sup> Here we tested whether this response extends to UV-B radiation as well. QRT-PCR revealed a significant decrease in *Slurp1* expression in the WT corneas 24 hours after UV-B exposure (Fig. 1A). Consistent with these results, immunofluorescent staining showed decreased expression of *Slurp1* in UV-B exposed WT corneas (Fig. 1B).

## A. qRT-PCR

B. Immunofluorescent staining (*Slurp1*, DAPI)

**FIGURE 1.** *Slurp1* expression decreases after UV-B irradiation. **(A)** qRT-PCR reveals a significant decrease in *Slurp1* transcripts in the eight-week-old 1350 J/m<sup>2</sup> UV-B-exposed WT mouse corneas compared with the untreated WT ( $n = 5$ ) ( $P = 0.001$ ). Error bars: the SEM. **(B)** Immunofluorescent staining confirmed decreased expression of *Slurp1* in the 1350 J/m<sup>2</sup> UV-B-exposed WT mouse CE compared with the untreated WT CE. No primary antibody control is shown. Magnification  $\times 60$ ; Scale bar: 20  $\mu\text{m}$  ( $n = 5$ ).

**SLURP1 Promotes Redox Homeostasis**

Different insults mentioned above that downregulate SLURP1 also cause ROS accumulation, implying that SLURP1 serves as an insult-agnostic immunomodulator by regulating redox homeostasis. To test this directly, we assessed the impact of SLURP1 on cellular redox status after UV-B exposure. GSH:GSSG ratio was used as a measure of oxidative stress, wherein a higher ratio indicates a healthier cellular redox state.<sup>29</sup> We subjected HCLE and HCLE-SLURP1 cells to UV-B radiation and measured the GSH/GSSG ratio after 24 hours. The GSH/GSSG ratio was 2- and  $\sim 2.5$ -fold higher in untreated HCLE-SLURP1-7 and HCLE-SLURP1-14 cells, respectively, compared with the control HCLE cells (Fig. 2A). UV-B exposure decreased the GSH/GSSG ratio across all cell lines, with the most reduction observed in HCLE cells. There was  $\sim 75\%$  decrease in HCLE cells, compared with  $\sim 31\%$  decrease in HCLE-SLURP1-7 cells and  $\sim 27\%$  decrease in HCLE-SLURP1-14 cells in the GSH/GSSG ratio, relative to their respective untreated control cells (Fig. 2A). Consistent with our earlier findings of comparable immune status in the naïve WT and *Slurp1X*<sup>-/-</sup> corneas,<sup>26</sup> there was no difference in their GSH:GSSG ratio (Fig. 2B). However, on UV-B irradiation, the *Slurp1X*<sup>-/-</sup> corneas showed a significantly lower GSH:GSSG ratio compared with the WT (Fig. 2B). Collectively, these results suggest that SLURP1 promotes corneal redox homeostasis.

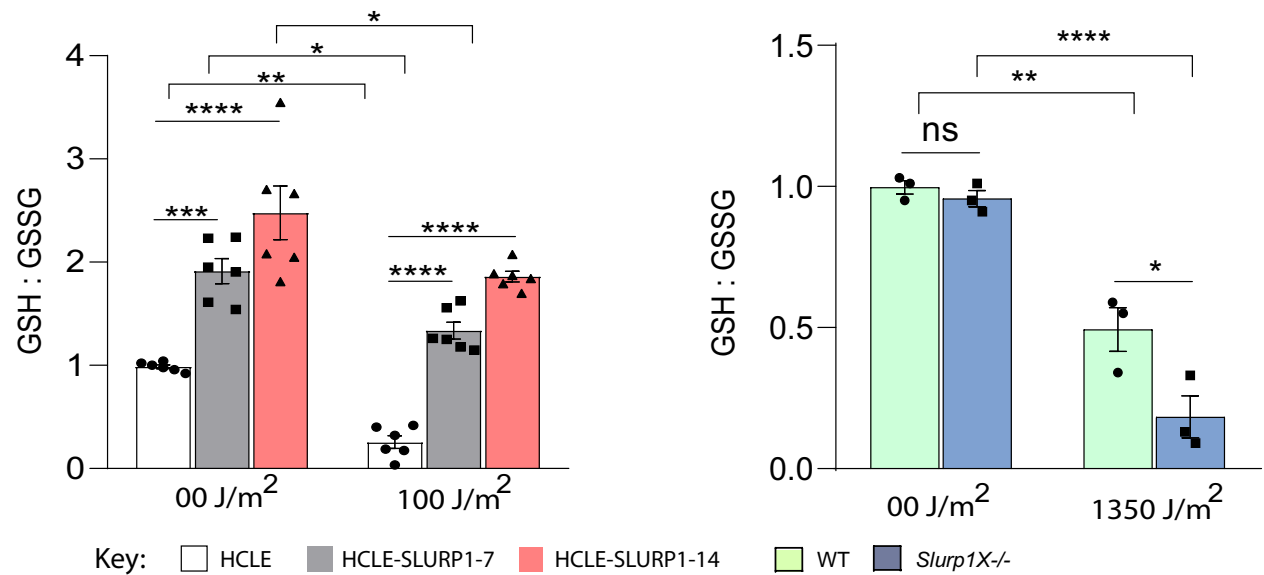
**SLURP1 Promotes Production of Anti-Oxidative Enzymes**

Next, we tested the effect of SLURP1 on GPX4, CAT and SOD2, the main anti-oxidative enzymes that help mitigate the harmful effects of ROS in oxidatively stressed cells.<sup>32</sup> *GPX4* gene expression at basal level was modestly elevated in HCLE-SLURP1-7 (1.14-fold) and HCLE-SLURP1-14 (1.46-fold) compared with HCLE cells (Fig. 3A). Six hours after UV-B exposure, *GPX4* expression significantly increased in the HCLE-SLURP1-7 (2.75-fold) and HCLE-SLURP1-14 (2.97-fold) cells compared with the HCLE cells (1.28-fold) (Fig. 3A). Similarly, *CAT* expression increased significantly in HCLE-SLURP1-7 (2.8-fold) and HCLE-SLURP1-14 (4.2-fold) compared with that in the HCLE cells (1.13-fold). *SOD2* followed the same trend with HCLE-SLURP1-7 (3.5-fold) and HCLE-SLURP1-14 (3.4-fold) showing a significant increase than the HCLE cells (1.6-fold) after UV-B exposure (Fig. 3A). As above, the naïve WT and *Slurp1X*<sup>-/-</sup> mouse corneas did not differ significantly in their expression of antioxidant enzymes (Fig. 3B). However, *Gpx4* expression decreased by 52% in the UV-B-irradiated *Slurp1X*<sup>-/-</sup> corneas compared with only 13% in the WT 24 hours after UV-B treatment (Fig. 3B). Both *Sod2* and *Cat* were downregulated by  $\sim 10$ – $20\%$  in UV-B-irradiated WT and *Slurp1X*<sup>-/-</sup> corneas (Fig. 3B). Collectively, these findings suggest that SLURP1 counteracts oxidative stress by enhancing the antioxidant defense systems.

**SLURP1 Suppresses ROS Accumulation**

ROS accumulation was quantified by measuring the DCF fluorescence intensity in the HCLE, HCLE-SLURP1-7 and HCLE-SLURP1-14 cells exposed to genotoxic stressors UV-B, MM-C, or H<sub>2</sub>O<sub>2</sub> that induce oxidative stress. At baseline, HCLE-SLURP1-7 and HCLE-SLURP1-14 cells accumu-

## A. Redox homeostasis in HCLE cells

B. Redox homeostasis in WT and *Slurp1X*<sup>-/-</sup> corneas

**FIGURE 2.** SLURP1 maintains redox homeostasis. GSH/GSSG ratio reveals the following: **(A)** more reduced environment in HCLE-SLURP1 cells in comparison with HCLE cells at baseline. 100 J/m<sup>2</sup> UV-B radiation decreased the GSH:GSSG ratio in all three cell lines. UV-B exposed HCLE-SLURP1 cells have a significantly higher GSH:GSSG ratio compared with HCLE cells, indicating the presence of more reduced glutathione in the presence of SLURP1 ( $n = 6$ ). **(B)** No difference in GSH:GSSG ratio in untreated WT and *Slurp1X*<sup>-/-</sup> mouse corneas. *Slurp1X*<sup>-/-</sup> corneas show significantly more decrease in GSH:GSSG ratio compared with WT corneas after 1350 J/m<sup>2</sup> UV-B, indicating the presence of more oxidized glutathione in the absence of Slurp1 ( $n = 3$ ). Error bars: SEM. (\* $P < 0.05$ , \*\* $P < 0.01$ , \*\*\* $P < 0.001$ , \*\*\*\* $P < 0.0001$ .)

lated  $-30\%$  and  $60\%$  less ROS, respectively, than the HCLE cells (Fig. 4A). HCLE-SLURP1-7 and HCLE-SLURP1-14 also accumulated significantly less ROS than the HCLE cells upon exposure to oxidative stressors UV-B radiation (Fig. 4A), MM-C (Fig. 4B), or H<sub>2</sub>O<sub>2</sub> (Fig. 4C). To mimic the physiological effect of secreted SLURP1 on the human ocular surface, we next tested the effect of CM collected from HCLE, HCLE-SLURP1-7, or HCLE-SLURP1-14 cell cultures on ROS accumulation in the HCLE cells. ELISA revealed that the HCLE-, HCLE-SLURP1-7- and HCLE-SLURP1-14-CM contained 1.0, 1.35, and 17.7 ng SLURP1, respectively, per mg of total protein (Fig. 4. D. i). At baseline, HCLE cells grown in HCLE-SLURP1-7 and HCLE-SLURP1-14 CM exhibited  $-32\%$  and  $46\%$  reduction in ROS accumulation, respectively, compared with those grown in HCLE CM. After exposure to UV-B, ROS levels increased 2.2-fold in HCLE cells grown in HCLE-CM, 1.6-fold in HCLE-SLURP1-7 CM, and 1.3-fold in HCLE-SLURP1-14 CM ( $P < 0.05$ ) (Fig. 4, D.ii). Consistent with these results, addition of increasing amounts of exogenous recombinant SLURP1 to the HCLE culture medium provided a dose-dependent protection from UV-B-induced ROS production (Fig. 4, D.iii). Collectively, these findings reveal that the extracellular SLURP1 suppresses intracellular ROS accumulation. Consistent with our previous findings and the results described above, ROS accumulation was comparable in the naïve WT and *Slurp1X*<sup>-/-</sup> corneas. On UV-B exposure, *Slurp1X*<sup>-/-</sup> corneas displayed a significantly higher increase in ROS levels (2.1-fold) compared with the WT (Fig. 4E), suggesting that Slurp1 plays a key role in preventing ROS accumulation in corneas exposed to oxidative stressors such as UV-B.

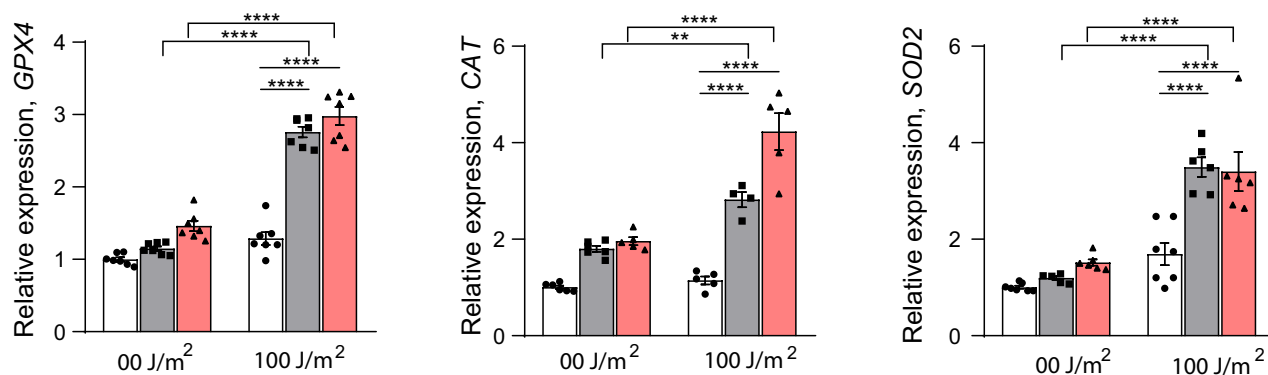
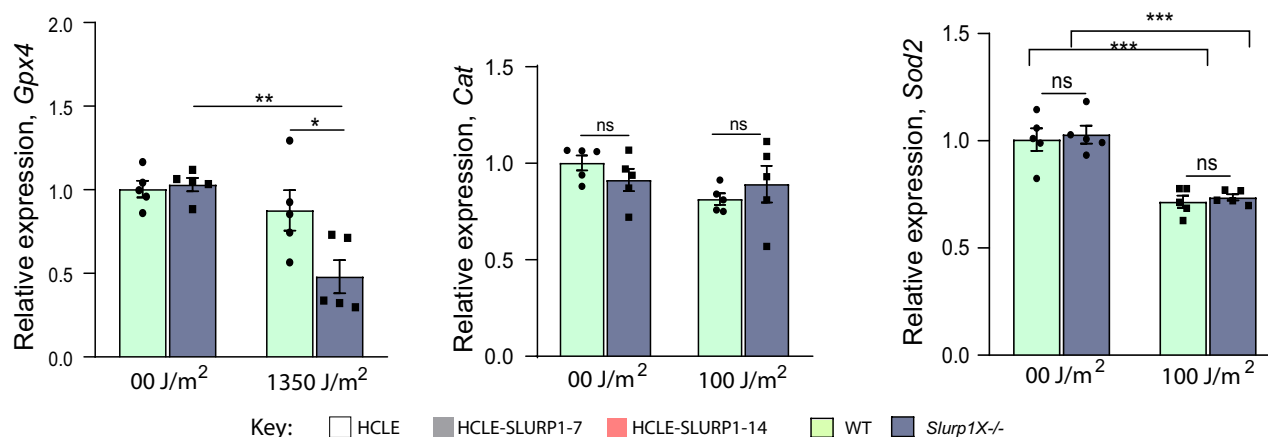
### SLURP1 Suppresses UV-B-Induced Lipid Peroxidation in HCLE Cells

Next, we investigated whether SLURP1 mitigates lipid peroxidation, one of the deleterious downstream effects of oxidative stress that produces highly reactive aldehydes such as 4-HNE and MDA.<sup>33,34</sup> Immunofluorescent staining revealed that HCLE-SLURP1-7 and HCLE-SLURP1-14 cells accumulate significantly less 4-HNE and MDA compared with HCLE cells 24 hours after UV-B exposure (Fig. 5). This was confirmed by radiometric analysis of lipid peroxidation using BODIPY C11 wherein UV-B-exposed HCLE cells showed a greater shift from red to green fluorescence compared with HCLE-SLURP1-7 and HCLE-SLURP1-14 cells, indicating higher lipid peroxidation in HCLE cells (Fig. 6). Collectively, these results elucidate that SLURP1 protects the cornea from harmful effects of the oxidative stress-induced lipid peroxidation.

### SLURP1 Protects the CE Cells From UV-B-Triggered DNA Damage

One of the more serious biological consequences of oxidative damage is mutagenic DNA double-strand breaks. We used  $\gamma$ -H2AX as a biomarker for oxidative stress-induced DNA double-strand breaks.<sup>35</sup> Immunofluorescent staining demonstrated a greater increase in the number of  $\gamma$ -H2AX-positive nuclei (and the intensity of staining) in control HCLE compared with the HCLE-SLURP1 cells after UV-B exposure (Fig. 7A). Next, we tested 8-OHdG—another specific marker of oxidative damage in both nuclear and mitochon-

## A. SLURP1 promotes expression of antioxidants in HCLE cells

B. *Slurp1X*<sup>-/-</sup> corneas display decreased expression of antioxidants

Key: □ HCLE ■ HCLE-SLURP1-7 ■ HCLE-SLURP1-14 □ WT ■ *Slurp1X*<sup>-/-</sup>

**FIGURE 3.** SLURP1 promotes antioxidant gene expression. The qRTPCR reveals the following: **(A)** Increased expression of antioxidant genes *GPX4*, *CAT* and *SOD2* in HCLE-SLURP1 compared with the HCLE cells after six hours of 100 J/m<sup>2</sup> UV-B exposure ( $n \geq 4$ ); **(B)** significant decrease in *Gpx4* expression in 1350 J/m<sup>2</sup> UV-B exposed *Slurp1X*<sup>-/-</sup> compared with the WT mouse cornea. There is no difference in catalase and SOD2 gene expression in the UV-B irradiated WT and *Slurp1X*<sup>-/-</sup> corneas ( $n = 5$ ). Error bars: SEM. (\* $P < 0.05$ , \*\* $P < 0.01$ , \*\*\* $P < 0.001$ , \*\*\*\* $P < 0.0001$ ).

drial DNA (mtDNA)—by immunofluorescent staining. More intense staining of 8-OHdG in the UV-B-exposed HCLE nucleus confirmed above findings with  $\gamma$ -H2AX, whereas the appearance of punctate staining in the HCLE cytoplasm suggested potential mtDNA damage in UV-B-exposed HCLE cells unlike that in the similarly treated HCLE-SLURP1 cells (Fig. 7B). Complementing this in vitro data, *Slurp1X*<sup>-/-</sup> mouse corneas exposed to single dose of UV-B (1350 J/m<sup>2</sup>) displayed a higher number of  $\gamma$ -H2AX-positive nuclei indicating increased DNA damage compared with the similarly treated WT corneas (Fig. 8). As earlier, there was no difference in the severity of DNA damage in the naïve WT and *Slurp1X*<sup>-/-</sup> corneas (Fig. 8). Collectively, these results elucidate that SLURP1 protects the cornea from oxidative stress-induced DNA damage.

### SLURP1 Prevents Oxidative Stress-Triggered Nuclear Localization of NF $\kappa$ B

Previously, we reported that SLURP1 stabilizes CE cell junctions and suppresses TNF $\alpha$ -induced cytokine production by suppressing nuclear localization of NF $\kappa$ B.<sup>27</sup> To determine if

SLURP1 protects the CE cells from oxidative stress-induced damage by a similar mechanism, we subjected HCLE and HCLE-SLURP1 cells at 70% confluence to (A) 0 J/m<sup>2</sup> or (B) 100 J/m<sup>2</sup> UV-B irradiation, allowed them to recover for four hours and performed immunofluorescent staining for NF $\kappa$ B and I $\kappa$ B (Fig. 9). A strong nuclear localization of NF $\kappa$ B was observed in UV-B-irradiated HCLE cells (Fig. 9, B.iii; arrowheads), unlike its predominantly cytoplasmic localization in the similarly treated HCLE-SLURP1 cells (Figs. 9, B.vi; Fig. 9, B.ix; arrows). HCLE-SLURP1 cells also displayed a modest increase in I $\kappa$ B staining intensity both before and after UV-B exposure (Fig. 9). Similar results were observed with NF $\kappa$ B and I $\kappa$ B in HCLE and HCLE-SLURP1 cells subjected to H<sub>2</sub>O<sub>2</sub>-mediated oxidative stress (Fig. 10). Collectively, these results suggest that SLURP1 protects the CE cells from oxidative stress-induced damage by preventing the nuclear localization of NF $\kappa$ B.

### DISCUSSION

Previously, we reported that SLURP1, highly expressed by the corneal epithelium and secreted into tear fluid, plays

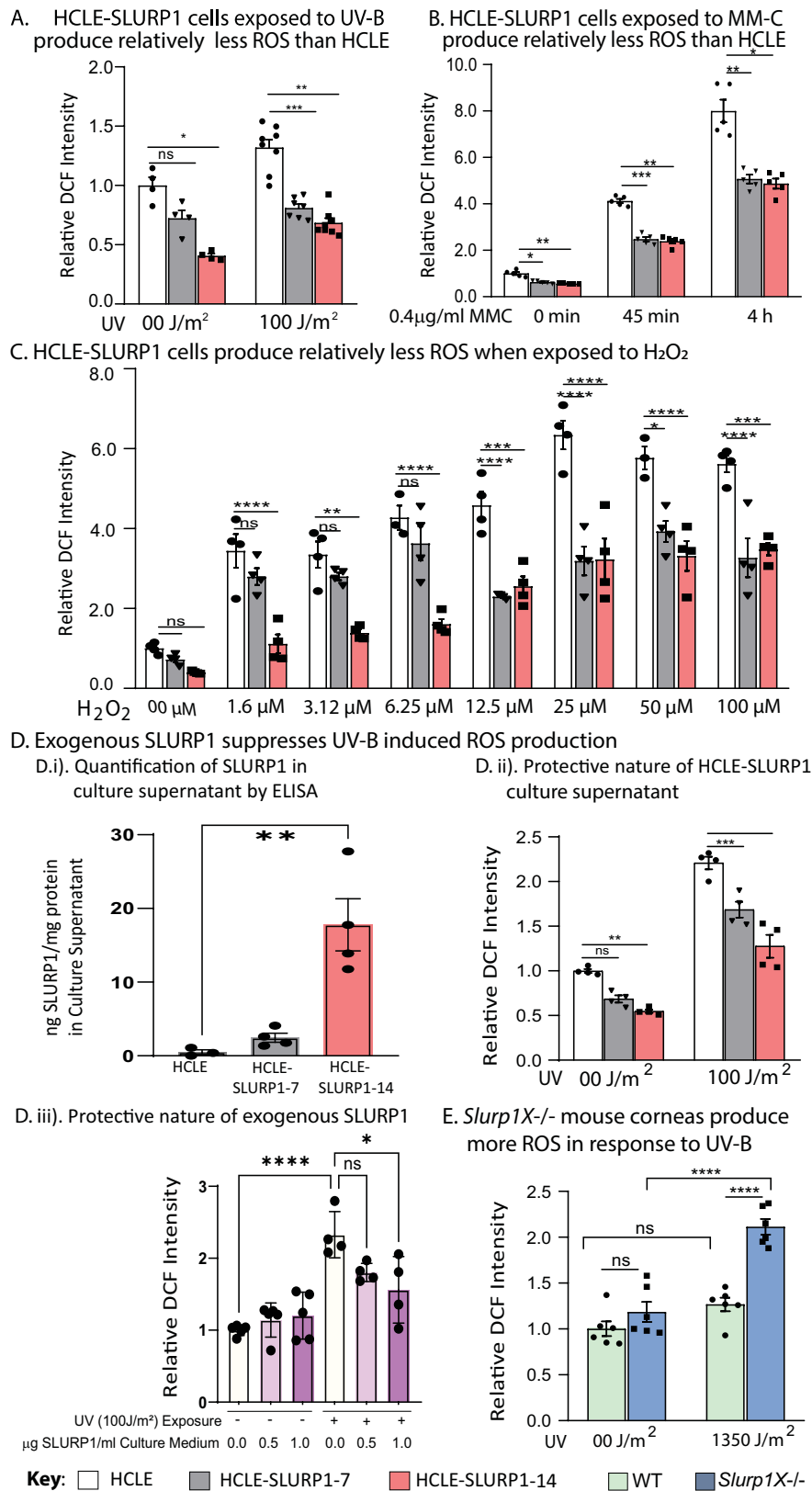


**FIGURE 4.** SLURP1 prevents accumulation of ROS. DCF intensity measurement reveals less ROS accumulation in HCLE-SLURP1 cells compared with the HCLE cells after (A) 100 J/m<sup>2</sup> UV-B (310 nm) exposure, (B) 0.4 μg/mL mitomycin-C treatment, and (C) H<sub>2</sub>O<sub>2</sub> (0–100 μM) treatment (n ≥ 4); (D) Exogenous SLURP1 protects HCLE cells from redox dysfunction by suppressing ROS accumulation. (D.i) Quantification of SLURP1 in HCLE and HCLE-SLURP1 cell culture supernatants by ELISA (n = 3). (D.ii) Protective effect of HCLE-SLURP1 culture supernatants on HCLE cells exposed to UV-B radiation (n = 4); (D.iii) Dose-dependent protective effect of exogenous recombinant SLURP1 on HCLE cells exposed to UV-B radiation (n = 4); (E) *Slurp1X*<sup>-/-</sup> mouse corneas accumulate more ROS than the WT after 1350 J/m<sup>2</sup> UV-B exposure (n = 6). Error bars: SEM. (\*P < 0.05; \*\*P < 0.01; \*\*\*P < 0.001; \*\*\*\*P < 0.0001.)

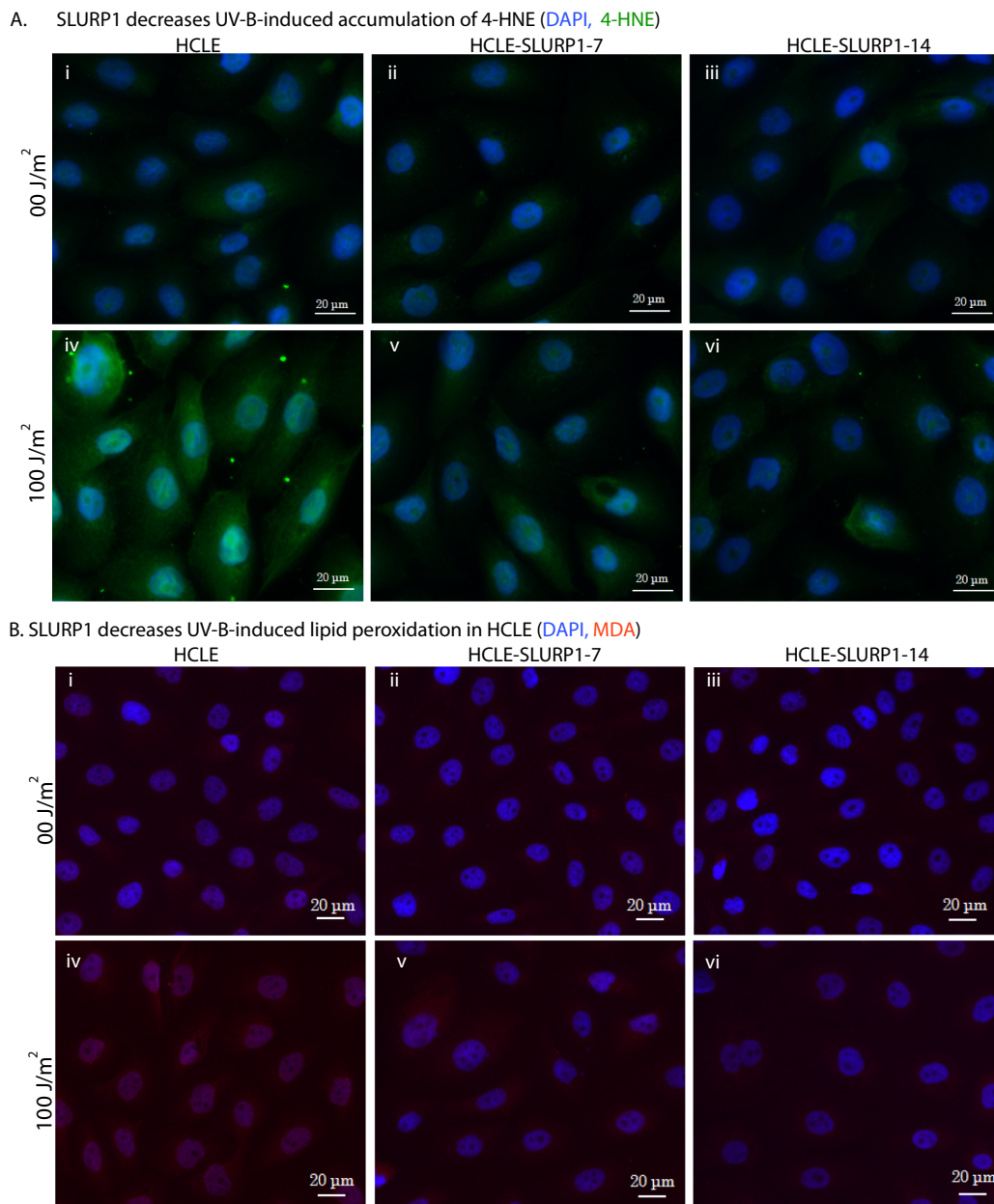


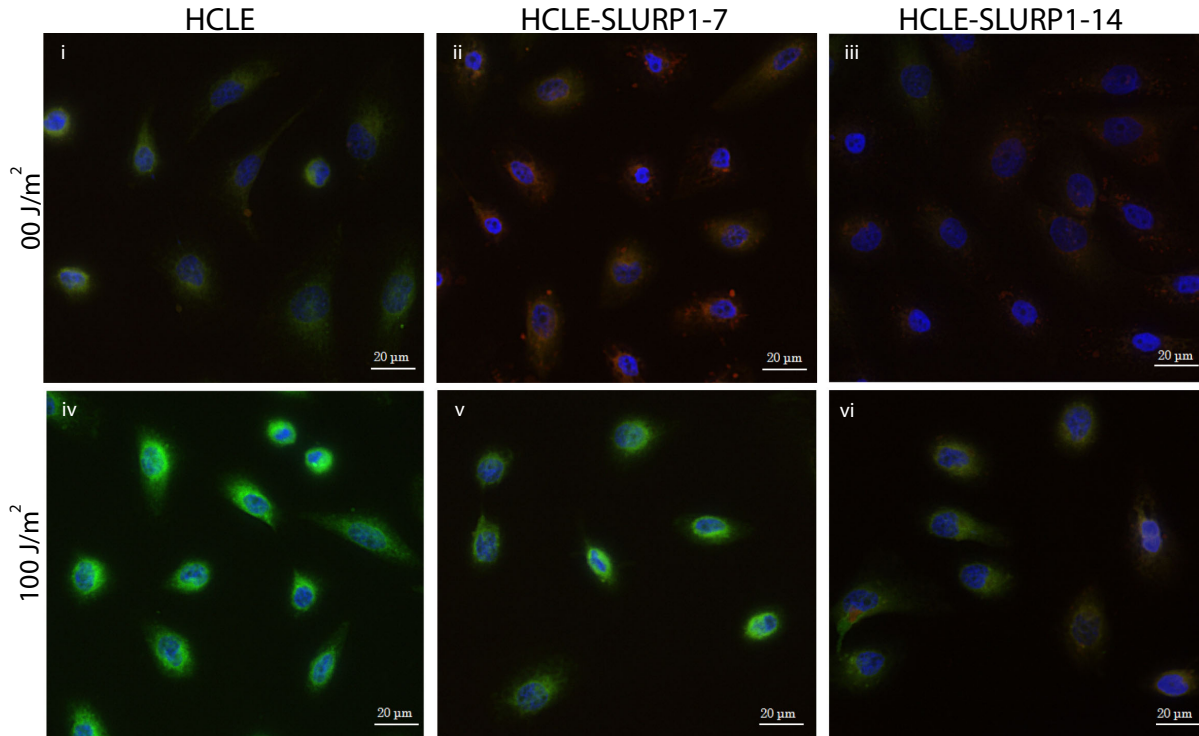
**FIGURE 5.** HCLE-SLURP1 cells display relatively less UV-B-induced lipid peroxidation than the HCLE cells. Immunofluorescent staining reveals relatively decreased accumulation of lipid peroxidation byproducts (A) 4-HNE and (B) MDA in HCLE-SLURP1 (v and vi) compared with the HCLE (iv) cells exposed to 100 J/m<sup>2</sup> UV-B radiation. Magnification  $\times 20$ ; scale bar: 20  $\mu\text{m}$ ,  $n = 3$ . No difference was noted between the untreated HCLE (i) and HCLE-SLURP1 (ii and iii) cells, in 4-HNE and MDA staining.

a key immunomodulatory role in the healthy cornea. In this report, considering that elevated oxidative stress is a common feature of the diverse proinflammatory conditions that downregulated SLURP1 expression allowing inflammation to progress further,<sup>10–11</sup> we tested whether SLURP1 plays a role in maintaining redox homeostasis. The data presented in this report elucidate that the SLURP1-overexpressing HCLE-SLURP1 cells display: (i) a better redox homeostasis with a healthier, more reduced environment; (ii) elevated expression of antioxidant enzymes; (iii) decreased intracellular ROS accumulation; (iv) decreased lipid peroxidation; (v) decreased nuclear and mitochondrial DNA damage relative to control HCLE cells; and (vi)

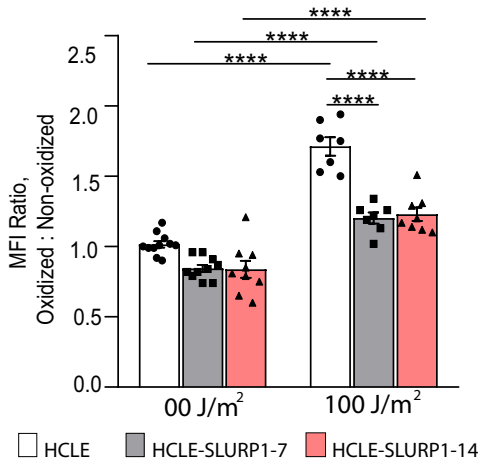
decreased nuclear localization of NF $\kappa$ B when exposed to oxidative stress. Additionally, *Slurp1* expression was downregulated in UV-B-exposed WT mouse corneas, and the UV-B-exposed *Slurp1X*<sup>–/–</sup> corneas exhibited higher ROS accumulation, greater DNA damage and reduced GPX4 levels compared with the WT corneas (Fig. 11). Overall, these findings support our hypothesis that “SLURP1 serves as an insult-agnostic immunomodulator by regulating redox homeostasis in corneal epithelial cells, thereby protecting the cornea from diverse genotoxic stressors” (Fig. 11).

An important finding in this study is that the WT and *Slurp1X*<sup>–/–</sup> corneas behave comparably in their

## A. SLURP1 decreases UV-B-induced lipid peroxidation in HCLE. (DAPI, BODIPY C11 Oxidized, Non-oxidized)



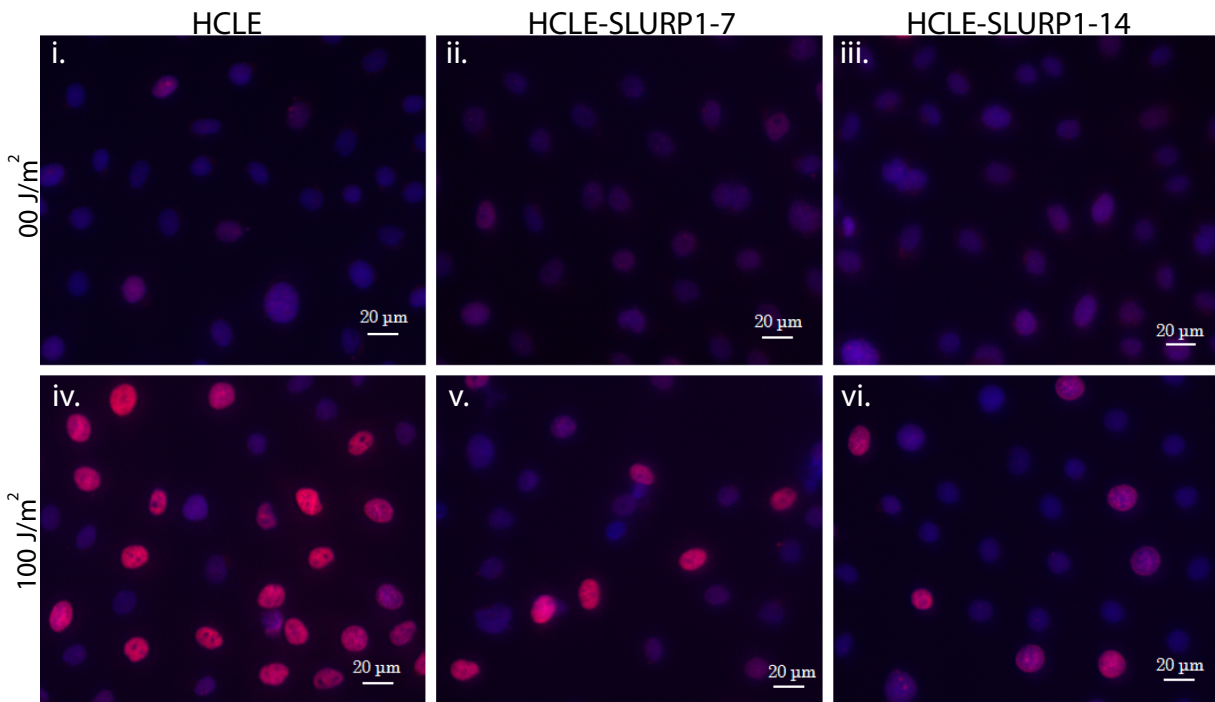
## B. BODIPY C11 Oxidized : Non-oxidized



**FIGURE 6.** HCLE-SLURP1 cells display less oxidized BODIPY C11 after UV-B exposure. **(A)** Compared with the untreated control HCLE (i), HCLE-SLURP1 (ii and iii) cells display relatively less oxidized BODIPY C11 (green) staining. In contrast, 100 J/m<sup>2</sup> UV-B-exposed HCLE cells (iv) display relatively more oxidized BODIPY C11 (green) than the HCLE-SLURP1 (v and vi) cells, indicating more lipid peroxidation in HCLE cells. Magnification  $\times 20$ ; scale bar: 20  $\mu\text{m}$ ;  $n = 3$ . **(B)** Mean fluorescence intensity (MFI) of oxidized (green) to nonoxidized (red) BODIPY C11 ( $n \geq 7$ ). Error bars: SEM. (\* $P < 0.05$ ; \*\* $P < 0.01$ ; \*\*\* $P < 0.001$ ; \*\*\*\* $P < 0.0001$ .)

naïve, unstressed state. However, when subjected to UV-B radiation-mediated oxidative stress, the *Slurp1X*<sup>-/-</sup> corneas display (i) relatively worse redox homeostasis; (ii) low level of antioxidant enzyme expression; (iii) higher ROS accumulation; and (iv) DNA damage, than the similarly treated WT. These results are consistent with our previous observations of enhanced corneal neovascularization in *Slurp1X*<sup>-/-</sup> corneas upon silver nitrate cautery<sup>18,26</sup> and elucidate that the *Slurp1X*<sup>-/-</sup> corneas are ill prepared to deal with oxidative stress.

GSH, a tripeptide composed of glutamate, cysteine, and glycine, functions as a key cellular redox buffer in conjunction with GSSG. It directly scavenges hydroxyl and superoxide radicals and acts as a cofactor for GPXs in metabolizing hydrogen peroxide and lipid peroxides. The cellular redox status, indicated by the GSH/GSSG ratio, is an important determinant of cell health.<sup>7,36,37</sup> UV-B exposure increases cellular oxidation, as evidenced by decrease in the GSH/GSSG ratio.<sup>38</sup> Our data elucidate that HCLE-SLURP1 cells maintain a higher GSH/GSSG ratio at baseline. Although there is a reduction in the GSH/GSSG ratio

A. SLURP1 decreases UV-B-induced accumulation of  $\gamma$ H2AX. (DAPI,  $\gamma$ H2AX)

## B. SLURP1 decreases UV-B-induced accumulation of 8-OHdG. (DAPI, 8-OHdG)

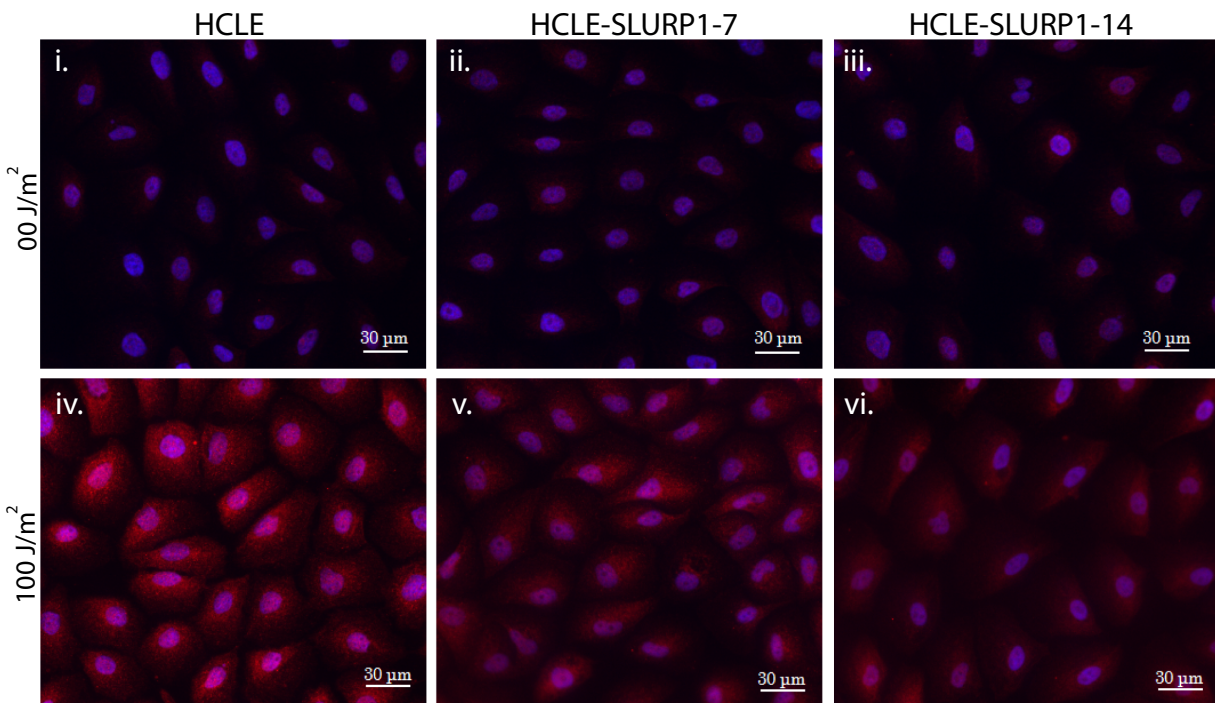


**FIGURE 7.** SLURP1 prevents UV-B-triggered DNA damage in HCLE cells. Immunofluorescent staining shows (A) fewer  $\gamma$ -H2AX positive nuclei (red) in UV-B ( $100 \text{ J/m}^2$ ) irradiated HCLE-SLURP1 cells (v and vi) compared with the similarly treated HCLE cells (iv). Magnification  $\times 20$ ; scale bar:  $20 \mu\text{m}$ ;  $n = 3$ ; and (B) relatively less 8-OHdG in the nuclei and cytoplasm of  $100 \text{ J/m}^2$  UV-B irradiated HCLE-SLURP1 (v and vi) compared with the similarly treated HCLE cells (iv). Evenly distributed 8-OHdG staining in the nuclei and punctate staining in the cytoplasm indicate nuclear and mitochondrial DNA damage, respectively. Magnification:  $\times 20$ ; scale bar:  $30 \mu\text{m}$ ,  $n = 3$ . No difference was noted between the untreated HCLE (i) and HCLE-SLURP1 (ii and iii) cells, in  $\gamma$ -H2AX and 8-OHdG staining.

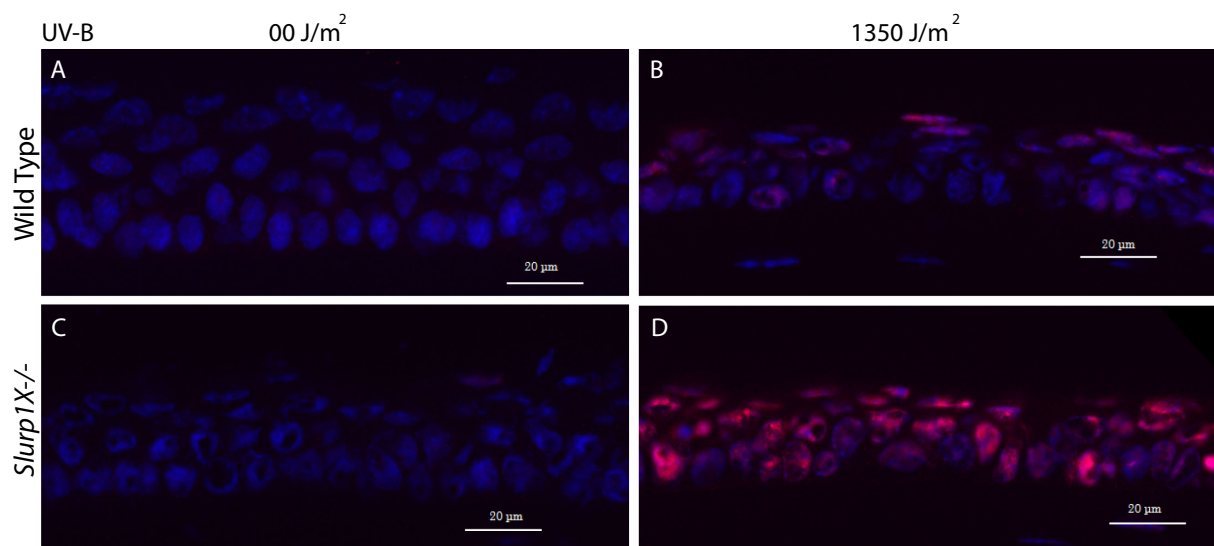


**FIGURE 8.** Increased UV-B-induced DNA damage in *Slurp1X*<sup>-/-</sup> corneas. Immunofluorescent staining shows a greater number of  $\gamma$ -H2AX positive nuclei (red) in 1350 J/m<sup>2</sup> UV-B irradiated *Slurp1X*<sup>-/-</sup> mouse CE (**D**) in comparison with the similarly treated WT mouse CE (**B**). Naïve WT and *Slurp1X*<sup>-/-</sup> mouse CE show no  $\gamma$ -H2AX-positive nuclei (**A** and **C**). Magnification:  $\times 60$ ; scale bar: 20  $\mu$ m,  $n = 5$ .

following 100 J/m<sup>2</sup> UV-B exposure, this decrease is more pronounced in HCLE cells compared with HCLE-SLURP1 cells, which continue to exhibit a higher GSH/GSSG ratio. These results demonstrate that SLURP1 plays a key role in cellular redox balance, thereby mitigating oxidative stress.

In response to UV-B-induced oxidative stress, the first-line antioxidant defense systems- GPXs, SODs, and CAT are activated to neutralize harmful ROS produced by the radiation.<sup>32</sup> GPX4, a membrane-bound enzyme, directly reduces lipid hydroperoxides. SODs convert two molecules of superoxide radical anions (O<sub>2</sub><sup>-</sup>) into H<sub>2</sub>O<sub>2</sub> and molecular oxygen (O<sub>2</sub>).<sup>39</sup> Catalase effectively catalyzes heterolytic cleavage of H<sub>2</sub>O<sub>2</sub> into oxygen and water, preventing ROS formation and maintaining cellular redox homeostasis. Our data presented in this report show that GPX4, CAT, and SOD2 are significantly upregulated in HCLE-SLURP1 compared with the HCLE cells. Antioxidant enzyme activity is decreased in response to radiation, implying that the body's ability to combat oxidative stress is decreased.<sup>40</sup> This was exaggerated in the UV-B exposed *Slurp1X*<sup>-/-</sup> corneas, which expressed much lower Gpx4 than the WT.

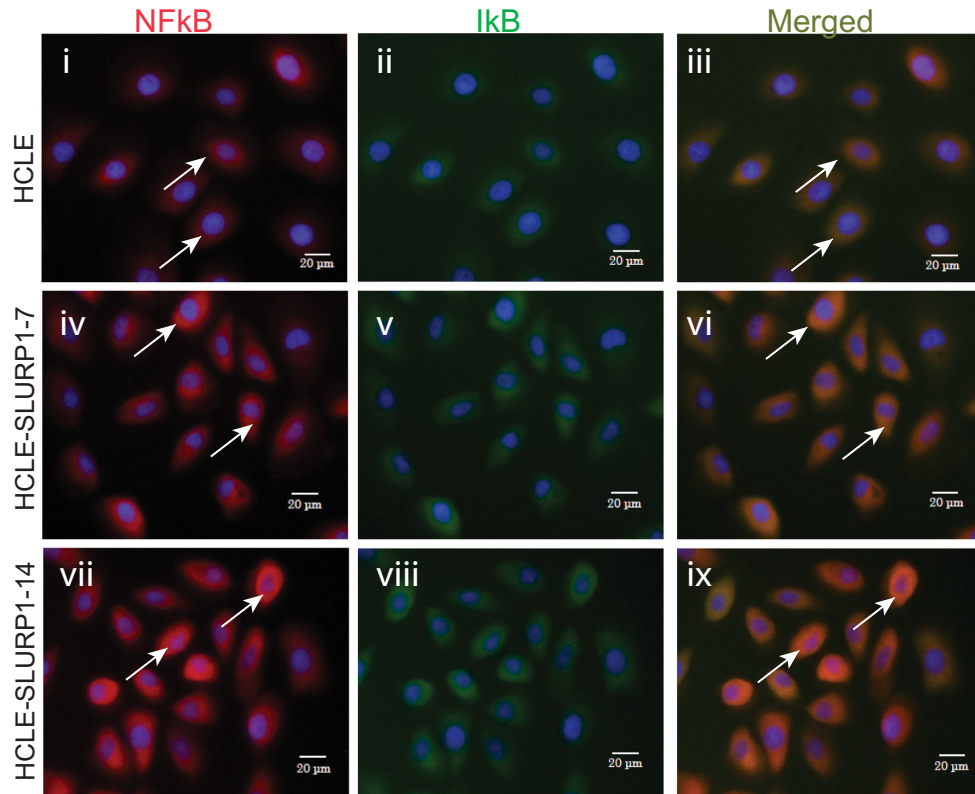
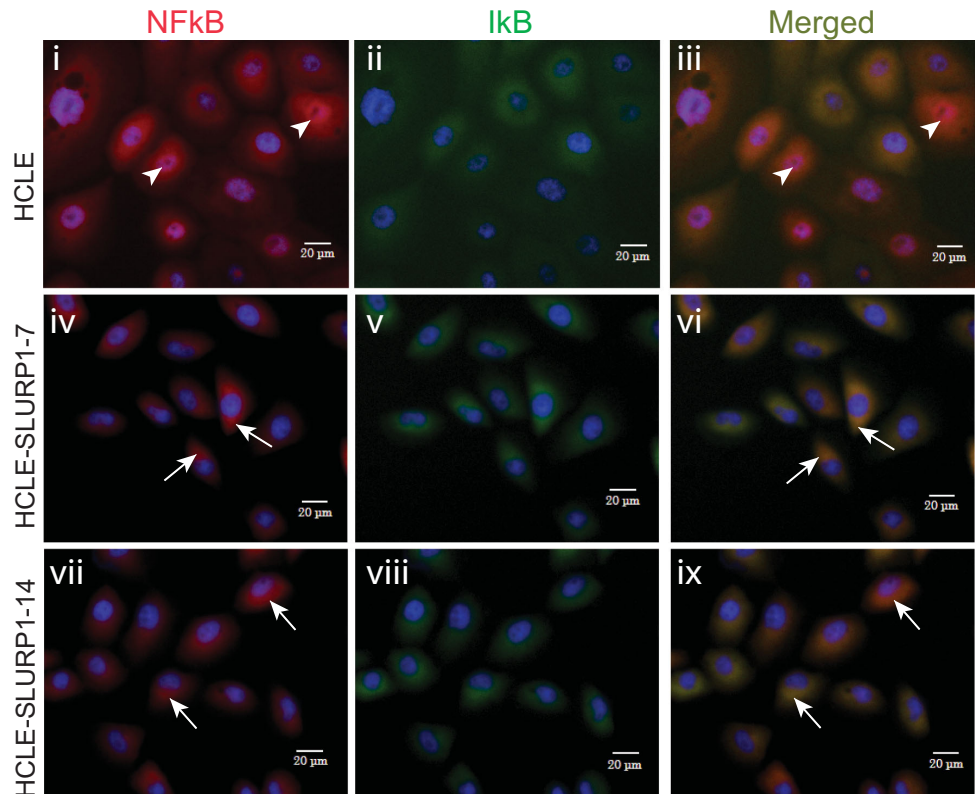
Lipid peroxidation is one of the most important downstream biological effects of excessive ROS accumulation. In the presence of elevated ROS, polyunsaturated fatty acid-rich membrane phospholipids are fragmented leading to formation of 4-HNE and MDA, major byproducts of lipid oxidation.<sup>41,42</sup> Elevated levels of 4-HNE cause NF- $\kappa$ B-mediated inflammation, protein and DNA damage, and mitochondrial dysfunction.<sup>42</sup> The data presented here demonstrate that the HCLE-SLURP1 cells display decreased 4-HNE and MDA staining and lower BODIPY C11 oxidized/reduced ratio consistent with decreased lipid peroxidation. These findings suggest that SLURP1 has a protective effect against UV-B-induced lipid peroxidation.

UV-B radiation indirectly damages DNA through the production of singlet oxygen or free radicals. Among ROS, the hydroxyl radical (OH<sup>\*</sup>) is particularly damaging because of its high reactivity with DNA.<sup>43</sup> Oxidative damage-induced modification of guanine to 8-Hydroxy-2'-

deoxyguanosine (8-OHdG) affects genomic stability, making 8-OHdG an important marker of oxidative DNA damage.<sup>44-46</sup> The data presented here with anti-8-OHdG antibody elucidate that the UV-B-exposed HCLE cells undergo more pronounced DNA damage than the similarly treated HCLE-SLURP1 cells. The punctate staining pattern of 8-OHdG in the cytoplasm of these cells indicates oxidative damage to mtDNA.<sup>47</sup> Additionally, nuclear staining for 8-OHdG was also more intense in HCLE cells exposed to UVB, suggesting a higher level of nuclear oxidative DNA damage in HCLE cells. We also assessed  $\gamma$ -H2AX, a well-established biomarker for DNA double-strand breaks, formed by phosphorylation of the Ser-139 residue of the histone variant H2AX.<sup>45</sup> We observed a higher number of  $\gamma$ -H2AX-positive nuclei in HCLE compared with HCLE-SLURP1 cells after UV-B exposure. Similarly, the  $\gamma$ -H2AX positive nuclei were more abundant in the UV-B exposed *Slurp1X*<sup>-/-</sup> corneas compared with WT corneas. Together, these results imply that SLURP1 protects the corneal epithelial cells from genotoxic stress-induced mitochondrial and nuclear DNA damage.

To summarize, the data presented here elucidate that SLURP1 protects the cornea from oxidative damage by promoting redox homeostasis in corneal epithelial cells that are frequently exposed to diverse oxidative stressors. SLURP1 achieves this by elevating the production of antioxidants and suppressing ROS accumulation. The improved redox homeostasis in the presence of SLURP1 further prevents the downstream effects of genotoxic oxidative stress such as lipid peroxidation and DNA damage. Together, these data elucidate the mechanistic basis for the broad insult-agnostic immunomodulatory role that SLURP1 plays in the cornea and identify SLURP1 as a valuable additive for artificial tear drops to provide enhanced protection from chronic dry eye disease-induced oxidative stress in the ocular surface (Fig. 11). The identity and specific nature of the cue(s) that elicit SLURP1 downregulation in proinflammatory conditions caused by different oxidative stressors remains to be determined.

## A. Control, 0 UV-B

B. 100 J/m<sup>2</sup> UV-B

**FIGURE 9.** SLURP1 suppresses UV-B-triggered nuclear localization of NF-κB. Immunofluorescent staining for NF-κB (red) and IκB (green) in HCLE, HCLE-SLURP1-7, and HCLE-SLURP1-14 cells at 70% confluence exposed to (A) 0 J/m<sup>2</sup> or (B) 100 J/m<sup>2</sup> UV-B irradiation and allowed to recover for four hours. The nuclear stain DAPI is depicted in blue color. The overlay images are shown in the right column. Arrowheads indicate nuclear localization of NF-κB in UV-B-irradiated HCLE cells, whereas the arrows point to the predominantly cytoplasmic localization of NF-κB in the similarly treated HCLE-SLURP1 cells. Scale bars: 20 μm. *n* = 3.

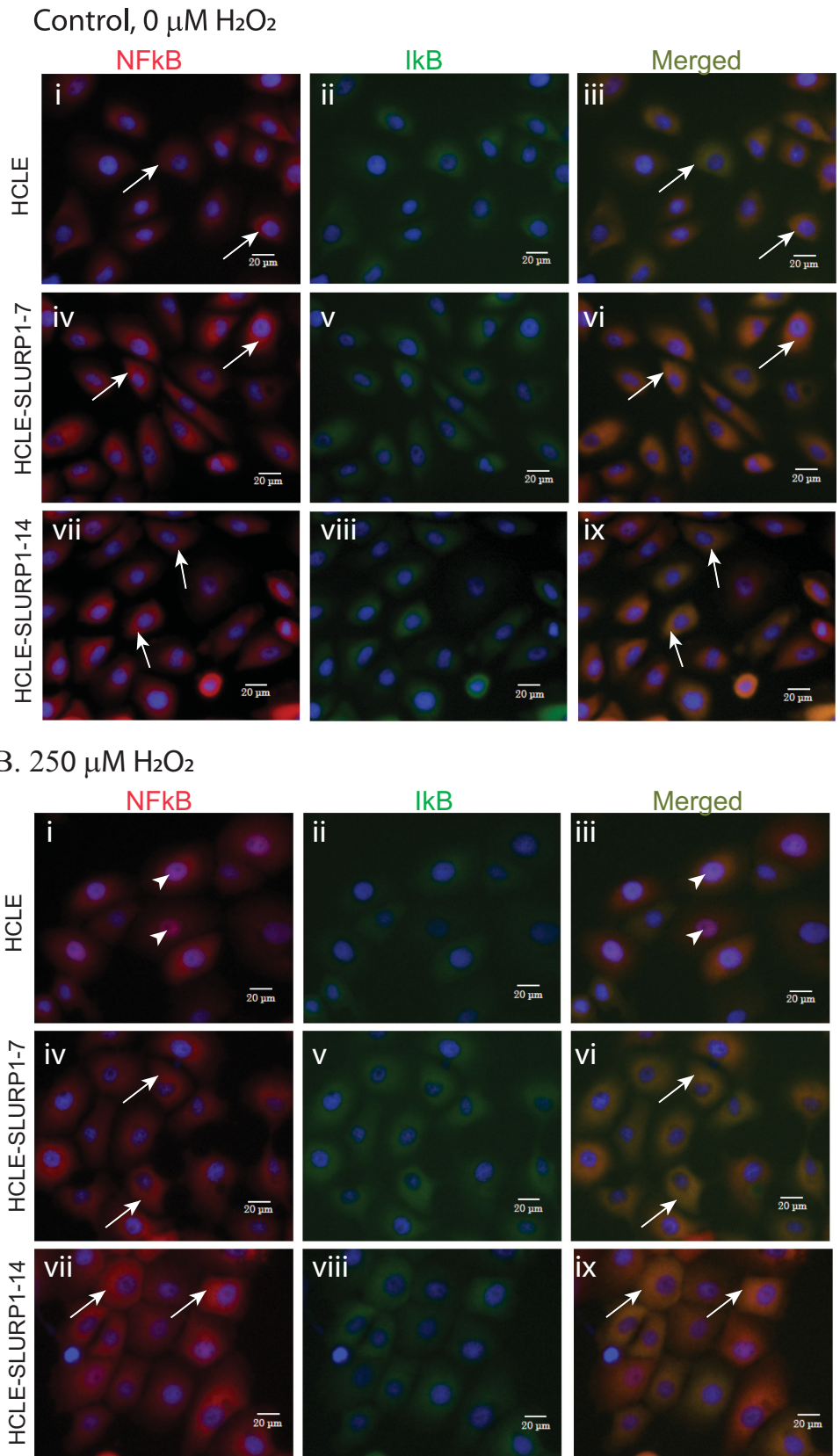


**FIGURE 10.** SLURP1 suppresses H<sub>2</sub>O<sub>2</sub>-triggered nuclear localization of NF- $\kappa$ B. Immunofluorescent staining for NF- $\kappa$ B (red) and I $\kappa$ B (green) in HCLE, HCLE-SLURP1-7, and HCLE-SLURP1-14 cells at 70% confluence exposed to (A) 0  $\mu$ M or (B) 250  $\mu$ M H<sub>2</sub>O<sub>2</sub> for one hour. The nuclear stain DAPI is depicted in blue. The overlay images are shown in the right column. Arrowheads indicate nuclear localization of NF- $\kappa$ B in H<sub>2</sub>O<sub>2</sub>-exposed HCLE cells, whereas the arrows point to the predominantly cytoplasmic localization of NF- $\kappa$ B in the similarly treated HCLE-SLURP1 cells. Scale bars: 20  $\mu$ m. *n* = 3.

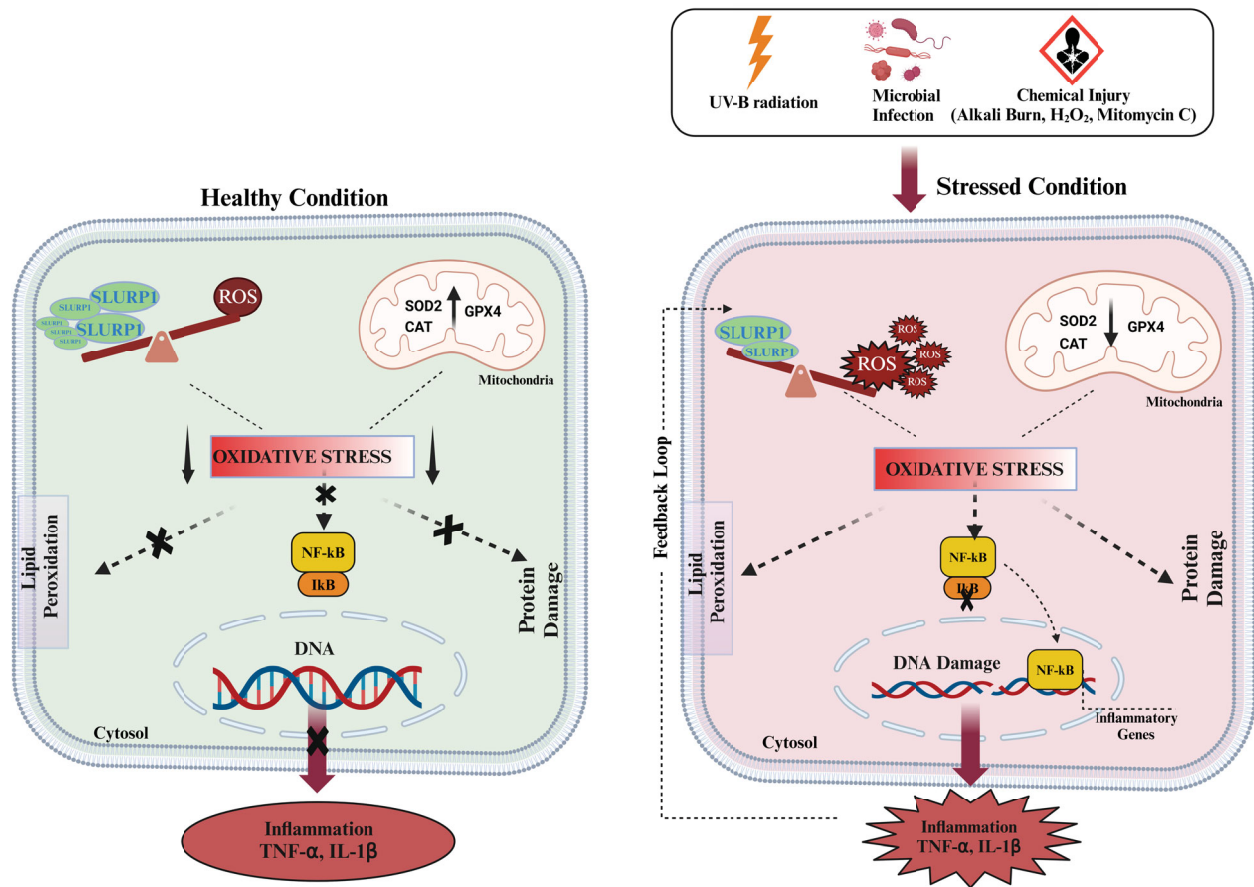


**FIGURE 11.** Schematic representation of the key findings in this study. The data presented in this report elucidate that upon UV-B exposure, the expression of SLURP1 decreases in WT mouse corneas. This results in an increase in ROS levels and decreased expression of antioxidant genes *Gpx4*, *Cat* and *Sod2*. This shift contributes to an increased oxidative stress and promotes (i) lipid peroxidation, as evidenced by increased 4-HNE and MDA; (ii) DNA damage, indicated by increased  $\gamma$ -H2AX and 8-OHdG, and (iii) Protein damage (inferred based on increased 4-HNE). Additionally, activation of NF- $\kappa$ B pathway leads to translocation of NF- $\kappa$ B into the nucleus, triggering activation of proinflammatory enzymes further escalating ROS production, creating a feedback loop. These results elucidate that SLURP1 protects the cornea from oxidative stress and identify SLURP1 as a potentially valuable additive for artificial tear drops to protect from chronic dry eye disease-induced oxidative stress in the ocular surface. The schematic figure was generated using BioRender software (BioRender, Toronto, ON, Canada).

### Acknowledgments

Supported by NEI grants RO1 EY026533, and RO1 EY031684. The funding agencies did not have any influence on design or conduct of the experiments described here, or preparation of this manuscript.

**Author Contributions:** First authors SK and PS designed and performed the experiments, prepared the figures and the first draft of the manuscript. SK, PS, SS, SK, and MV performed the experiments and analyzed the data presented. SKS conceived the study, provided the reagents, and oversaw the project. All authors helped prepare the manuscript and have read the last version of the submitted manuscript and agree with its publication.

**Disclosure:** **S. Kaur**, The Secreted Ly6/uPAR-Related Protein-1 (SLURP1) Protects the Cornea from Oxidative Stress (P); **P. Sohnen**, None; **S. Kumar**, None; **M. Vohra**, None; **Sudha Swamynathan**, Use of SLURP1 as an Immunomodulatory Molecule in the Ocular Surface (P), The Secreted Ly6/uPAR-Related Protein-1 (SLURP1) Protects the Cornea from Oxidative Stress (P); **Shivalingappa Swamynathan**, Use of SLURP1 as an Immunomodulatory Molecule in the Ocular Surface (P),

The Secreted Ly6/uPAR-Related Protein-1 (SLURP1) Protects the Cornea from Oxidative Stress (P)

### References

1. Kaur S, Sohnen P, Swamynathan S, Du Y, Espana EM, Swamynathan SK. Molecular nature of ocular surface barrier function, diseases that affect it, and its relevance for ocular drug delivery. *Ocul Surf.* 2023;30:3–13.
2. Shoham A, Hadziahmetovic M, Dunaief JL, Mydlarski MB, Schipper HM. Oxidative stress in diseases of the human cornea. *Free Radic Biol Med.* 2008;45:1047–1055.
3. Chen X, Yang J, Li M, et al. Fullereneol protects cornea from ultraviolet B exposure. *Redox Biol.* 2022;54:102360.
4. Delic NC, Lyons JG, Di Girolamo N, Halliday GM. Damaging effects of ultraviolet radiation on the cornea. *Photochem Photobiol.* 2017;93:920–929.
5. Jiang GJ, You XG, Fan TJ. Ultraviolet B irradiation induces senescence of human corneal endothelial cells in vitro by DNA damage response and oxidative stress. *J Photochem Photobiol B.* 2022;235:112568.
6. Lingappan K. NF- $\kappa$ B in oxidative stress. *Curr Opin Toxicol.* 2018;7:81–86.

7. Chen Y, Mehta G, Vasiliou V. Antioxidant defenses in the ocular surface. *Ocul Surf.* 2009;7:176–185.
8. Chen Y, Thompson DC, Koppaka V, Jester JV, Vasiliou V. Ocular aldehyde dehydrogenases: protection against ultraviolet damage and maintenance of transparency for vision. *Prog Retin Eye Res.* 2013;33:28–39.
9. Böhm EW, Buonfiglio F, Voigt AM, et al. Oxidative stress in the eye and its role in the pathophysiology of ocular diseases. *Redox Biol.* 2023;68:102967.
10. Swamynathan S, Buella KA, Kinchington P, et al. Klf4 regulates the expression of Slurp1, which functions as an immunomodulatory peptide in the mouse cornea. *Invest Ophthalmol Vis Sci.* 2012;53:8433–8446.
11. Swamynathan S, Delp EE, Harvey SA, Loughner CL, Raju L, Swamynathan SK. Corneal expression of SLURP-1 by age, sex, genetic strain, and ocular surface health. *Invest Ophthalmol Vis Sci.* 2015;56:7888–7896.
12. Moriwaki Y, Yoshikawa K, Fukuda H, Fujii YX, Misawa H, Kawashima K. Immune system expression of SLURP-1 and SLURP-2, two endogenous nicotinic acetylcholine receptor ligands. *Life sciences.* 2007;80:2365–2368.
13. Arredondo J, Chernyavsky AI, Grando SA. SLURP-1 and -2 in normal, immortalized and malignant oral keratinocytes. *Life sciences.* 2007;80:2243–2247.
14. Favre B, Plantard L, Aeschbach L, et al. SLURP1 is a late marker of epidermal differentiation and is absent in Mal de Meleda. *J Invest Dermatol.* 2007;127:301–308.
15. Ertle CM, Rommel FR, Tumala S, et al. New pathways for the skin's stress response: the cholinergic neuropeptide SLURP-1 can activate mast cells and alter cytokine production in mice. *Front Immunol.* 2021;12:631881.
16. Swamynathan S, Campbell G, Tiwari A, Swamynathan SK. Secreted Ly-6/uPAR-related protein-1 (SLURP1) is a pro-differentiation factor that stalls G1-S transition during corneal epithelial cell cycle progression. *Ocul Surf.* 2022;24:1–11.
17. Swamynathan S, Swamynathan SK. SLURP-1 modulates corneal homeostasis by serving as a soluble scavenger of urokinase-type plasminogen activator. *Invest Ophthalmol Vis Sci.* 2014;55:6251–6261.
18. Swamynathan S, Loughner CL, Swamynathan SK. Inhibition of HUVEC tube formation via suppression of NFκB suggests an anti-angiogenic role for SLURP1 in the transparent cornea. *Exp Eye Res.* 2017;164:118–128.
19. Swamynathan S, Tiwari A, Loughner CL, et al. The secreted Ly6/uPAR-related protein-1 suppresses neutrophil binding, chemotaxis, and transmigration through human umbilical vein endothelial cells. *Sci Rep.* 2019;9:5898.
20. Grando SA. Basic and clinical aspects of non-neuronal acetylcholine: biological and clinical significance of non-canonical ligands of epithelial nicotinic acetylcholine receptors. *J Pharmacol Sci* 2008;106:174–179.
21. Lyukmanova EN, Shulepko MA, Kudryavtsev D, et al. Human secreted Ly-6/uPAR related protein-1 (SLURP-1) is a selective allosteric antagonist of alpha7 nicotinic acetylcholine receptor. *PLoS One.* 2016;11:e0149733.
22. Lyukmanova EN, Bychkov ML, Sharonov GV, et al. Human secreted proteins SLURP-1 and SLURP-2 control the growth of epithelial cancer cells via interactions with nicotinic acetylcholine receptors. *Br J Pharmacol.* 2018;175:1973–1986.
23. Jia C, Zhu W, Ren S, Xi H, Li S, Wang Y. Comparison of genome-wide gene expression in suture- and alkali burn-induced murine corneal neovascularization. *Mol Vis.* 2011;17:2386–2399.
24. Oszejka K, Bieniasz M, Brown G, Swiatkowska M, Bartkowiak J, Szemraj J. Effect of oxidative stress on the expression of t-PA, u-PA, u-PAR, and PAI-1 in endothelial cells. *Biochem Cell Biol.* 2008;86:477–486.
25. Swamynathan S, Loughner CL, Swamynathan SK. Inhibition of HUVEC tube formation via suppression of NFκB suggests an anti-angiogenic role for SLURP1 in the transparent cornea. *Exp Eye Res.* 2017;164:118–128.
26. Swamynathan S, Campbell G, Sohnen P, Kaur S, St Leger AJ, Swamynathan SK. The secreted Ly6/uPAR-related protein 1 (SLURP1) modulates corneal angiogenic inflammation via NF-κB signaling. *Invest Ophthalmol Vis Sci.* 2024;65:37.
27. Campbell G, Swamynathan S, Tiwari A, Swamynathan SK. The secreted Ly-6/uPAR related protein-1 (SLURP1) stabilizes epithelial cell junctions and suppresses TNF-alpha-induced cytokine production. *Biochem Biophys Res Commun.* 2019;517:729–734.
28. Adeyo O, Allan BB, Barnes RH, 2nd, et al. Palmoplantar keratoderma along with neuromuscular and metabolic phenotypes in Slurp1-deficient mice. *J Invest Dermatol.* 2014;134:1589–1598.
29. Giustarini D, Colombo G, Garavaglia ML, et al. Assessment of glutathione/glutathione disulphide ratio and S-glutathionylated proteins in human blood, solid tissues, and cultured cells. *Free Radic Biol Med.* 2017;112:360–375.
30. Gupta D, Harvey SA, Kenchegowda D, Swamynathan S, Swamynathan SK. Regulation of mouse lens maturation and gene expression by Kruppel-like factor 4. *Exp Eye Res.* 2013;116:205–218.
31. Kim DH, Im S-T, Yoon JY, et al. Comparison of therapeutic effects between topical 8-oxo-2'-deoxyguanosine and corticosteroid in ocular alkali burn model. *Sci Rep.* 2021;11:6909.
32. Jomova K, Alomar SY, Alwasel SH, Nepovimova E, Kuca K, Valko M. Several lines of antioxidant defense against oxidative stress: antioxidant enzymes, nanomaterials with multiple enzyme-mimicking activities, and low-molecular-weight antioxidants. *Arch Toxicol.* 2024;98:1323–1367.
33. Ayala A, Muñoz MF, Argüelles S. Lipid peroxidation: production, metabolism, and signaling mechanisms of malondialdehyde and 4-hydroxy-2-nonenal. *Oxid Med Cell Longev.* 2014;2014:360438.
34. Houghlum K, Filip M, Witztum JL, Chojkier M. Malondialdehyde and 4-hydroxynonenal protein adducts in plasma and liver of rats with iron overload. *J Clin Invest.* 1990;86:1991–1998.
35. Podhorecka M, Skladanowski A, Bozko P. H2AX Phosphorylation: its role in DNA damage response and cancer therapy. *J Nucleic Acids.* 2010;2010:920161.
36. Chen Y, Shertzer HG, Schneider SN, Nebert DW, Dalton TP. Glutamate cysteine ligase catalysis: dependence on ATP and modifier subunit for regulation of tissue glutathione levels. *J Biol Chem.* 2005;280:33766–33774.
37. Arthur JR. The glutathione peroxidases. *Cell Mol Life Sci.* 2000;57:1825–1835.
38. Kim S, You DH, Han T, Choi EM. Modulation of viability and apoptosis of UVB-exposed human keratinocyte HaCaT cells by aqueous methanol extract of laver (*Porphyra yezoensis*). *J Photochem Photobiol B.* 2014;141:301–307.
39. Brigelius-Flohé R, Maiorino M. Glutathione peroxidases. *Biochim Biophys Acta.* 2013;1830:3289–3303.
40. Rezaeyan A, Haddadi GH, Hosseinzadeh M, Moradi M, Najafi M. Radioprotective effects of hesperidin on oxidative damages and histopathological changes induced by X-irradiation in rats heart tissue. *J Med Phys.* 2016;41:182–191.
41. Li Y, Zhao T, Li J, et al. Oxidative stress and 4-hydroxy-2-nonenal (4-HNE): implications in the pathogenesis and treatment of aging-related diseases. *J Immunol Res.* 2022;2022:2233906.
42. Stasiewicz A, Conde T, Gęgotek A, Domingues MR, Domingues P, Skrzydlewska E. Prevention of UVB induced metabolic changes in epidermal cells by lipid extract

- from microalgae nannochloropsis oceanica. *Int J Mol Sci.* 2023;24:11302.
43. Hernández AR, Vallejo B, Ruzgas T, Björklund S. The effect of UVB irradiation and oxidative stress on the skin barrier-a new method to evaluate sun protection factor based on electrical impedance spectroscopy. *Sensors (Basel).* 2019;19:2376.
44. Cadet J, Douki T, Ravanat JL. Oxidatively generated base damage to cellular DNA. *Free Radic Biol Med.* 2010;49:9-21.
45. Kciuk M, Marciniak B, Mojzych M, Kontek R. Focus on UV-Induced DNA Damage and Repair-Disease Relevance and Protective Strategies. *Int J Mol Sci.* 2020;21:7264.
46. Omari Shekaftik S, Nasirzadeh N. 8-Hydroxy-2'-deoxyguanosine (8-OHdG) as a biomarker of oxidative DNA damage induced by occupational exposure to nanomaterials: a systematic review. *Nanotoxicology.* 2021;15:850-864.
47. Joyce NC, Zhu CC, Harris DL. Relationship among oxidative stress, DNA damage, and proliferative capacity in human corneal endothelium. *Invest Ophthalmol Vis Sci.* 2009;50:2116-2122.